

Results on Hard Diffractive Production

Konstantin Goulianos¹

*The Rockefeller University
New York, NY 10021, USA
(The CDF Collaboration)*

The results of experiments at hadron colliders probing the structure of the pomeron through hard diffraction are reviewed. Some results on deep inelastic diffractive scattering obtained at HERA are also discussed and placed in perspective. By using a properly normalized pomeron flux factor in single diffraction dissociation, as dictated by unitarity, the pomeron emerges as a combination of valence quark and gluon color singlets in a ratio suggested by asymptopia.

I. INTRODUCTION

In this paper we review results obtained in studies of hard diffractive production at hadron colliders and deep inelastic diffractive scattering at HERA and draw conclusions about the QCD structure of the pomeron. The results on diffractive W and dijet production are presented on behalf of the CDF Collaboration.

The phenomenology associated with extracting information on the pomeron structure from these studies relies on Regge theory and factorization.

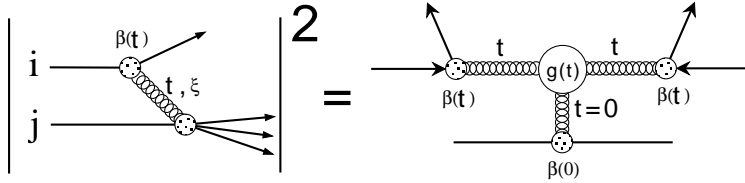


FIG. 1. The triple-pomeron amplitude for single diffraction dissociation.

The cross section for single diffraction dissociation in Regge theory has the form (see Fig. 1)

$$\frac{d^2\sigma_{sd}^{ij}}{dt d\xi} = \frac{1}{16\pi} \frac{\beta_{iP}^2(t)}{\xi^{2\alpha(t)-1}} \left[\beta_{jP}(0) g(t) \left(\frac{s'}{s_0} \right)^{\alpha(0)-1} \right] = f_{P/i}(\xi, t) \sigma_T^{Pj}(s', t) \quad (1)$$

¹Presented at the 10th Topical Workshop on Proton-Antiproton Collider Physics, 9-13 May 1995, Fermi National Accelerator Laboratory.

where \mathcal{P} stands for pomeron, s' is the s-value in the $\mathcal{P} - j$ reference frame, s'_0 is a constant conventionally set to 1 GeV², $\xi = s'/s$ is the Feynman- x of the pomeron in hadron- i , and $\alpha(t)$ the pomeron trajectory given by $\alpha(t) = \alpha(0) + \alpha't = 1 + \epsilon + \alpha't$. The term in the square brackets is interpreted as the total cross section of the pomeron on hadron- j , $\sigma_T^{\mathcal{P}j}(s', t)$, where $g(t)$ is the “triple-pomeron coupling constant”. This interpretation leads naturally to viewing single diffraction as being due to a flux of pomerons, $f_{\mathcal{P}/i}(\xi, t)$, emitted by hadron- i and interacting with hadron- j .

Assuming that factorization holds in *hard* processes, as it does in soft (1), Ingelman and Schlein (IS) used the pomeron flux from Eq. 1 to calculate high- P_T jet production in $p\bar{p}$ single diffraction dissociation (2). Their calculation was followed by the discovery of diffractive dijets by UA8 (3). However, the measured dijet rate turned out to be substantially lower than the rate predicted by the IS model (4). One possible explanation for this result is that the *virtual* pomeron does not obey the momentum sum rule (4,5). A more physical explanation, in which the pomeron *obeys* the momentum sum rule, is offered by extending the IS model to interpret the pomeron flux as a probability density for finding a pomeron inside hadron- i and *renormalizing* it so that it is not allowed to exceed unity (6). As we shall see below, using a renormalized pomeron flux lowers the predicted rates and brings the UA8 results into agreement with the momentum sum rule.

The pomeron flux renormalization procedure was proposed in order to unitarize single diffraction dissociation. Without renormalization, the $p\bar{p}$ single diffractive cross section rises much faster than that observed, reaching the total cross section and therefore violating unitarity at the TeV energy scale. The renormalized flux is given by

$$f_N(\xi, t) = \frac{f_{\mathcal{P}/i}(\xi, t)d\xi dt}{N(\xi_{min})} \quad (2)$$

$$N(\xi_{min}) \equiv \begin{cases} 1 & \text{if } N(\xi_{min}) \leq 1 \\ \int_{\xi_{min}}^{0.1} d\xi \int_{t=0}^{\infty} f_{\mathcal{P}/i}(\xi, t) dt & \text{if } N(\xi_{min}) > 1 \end{cases}$$

where $\xi_{min} = (1.5 \text{ GeV}^2/s)$ for $p\bar{p}$ soft single diffraction (6). Below, experimental results on hard diffraction will be compared with predictions obtained both with the standard and with the renormalized pomeron flux.

II. HARD DIFFRACTION AT HADRON COLLIDERS

Events are tagged as diffractive either by the detection of a high- x_F (anti)proton, which presumably “emitted” a small- ξ pomeron, or by the presence of a rapidity gap at one end of the kinematic region, as shown in Fig. 2.

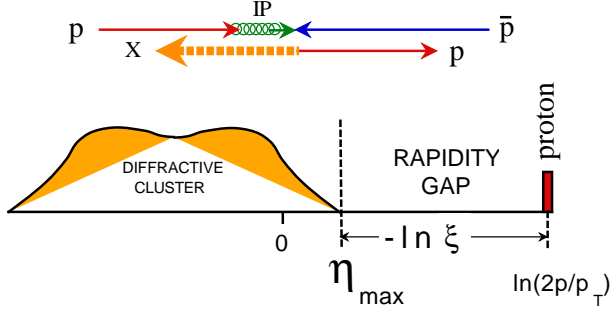


FIG. 2. Pseudorapidity distribution of particles in diffraction dissociation.

A. The UA8 experiment

UA8 pioneered hard diffraction studies by observing high- P_T jet production in the process $p + \bar{p} \rightarrow p + Jet_1 + Jet_2 + X$ at the CERN $S\bar{p}\bar{p}S$ collider at $\sqrt{s} = 630$ GeV. Events with two jets of $P_T > 8$ GeV were detected in coincidence with a high- x_F proton, whose momentum and angle were measured in a forward “roman pot” spectrometer. The event sample spanned the kinematic range $0.9 < x_p < 0.94$ and $0.9 < |t| < 2.3$ GeV². By comparing the x_F distribution of the sum of the jet momenta in the pomeron-proton rest frame with Monte Carlo distributions generated with different pomeron structure functions, UA8 concluded (3) that the partonic structure of the pomeron is $\sim 57\%$ *hard* [$6\beta(1 - \beta)$], $\sim 30\%$ *superhard* [$\delta(\beta)$], and $\sim 13\%$ *soft* [$6(1 - \beta)^5$]. However, the measured dijet production rate was found to be smaller than that predicted for a hard-quark(gluon) pomeron obeying the momentum sum rule by a “discrepancy factor” of $0.46 \pm 0.08 \pm 0.24$ ($0.19 \pm 0.03 \pm 0.10$) (4). Using the renormalized pomeron flux, the discrepancy factor becomes $1.79 \pm 0.31 \pm 0.93$ ($0.74 \pm 0.11 \pm 0.39$) (6), which is consistent with the momentum sum rule.

B. Diffractive W's in CDF

The quark content of the pomeron can be probed directly with diffractive W production, which to leading order occurs through $q\bar{q} \rightarrow W$. A hard gluonic pomeron can also lead to diffractive W 's through $gq \rightarrow Wq(\rightarrow W + Jet)$, but the rate for this subprocess is down by a factor of order α_s . The ratio of diffractive to non-diffractive $W^\pm(\rightarrow l^\pm\nu)$ production has been calculated by Bruni and Ingelman (BI) (7) to be $\sim 17\%$ ($\sim 1\%$) for a hard-quark(gluon), and $\sim 0.4\%$ for a soft-quark pomeron structure. Thus, diffractive W production is mainly sensitive to the hard-quark component of the pomeron structure

function. However, using the renormalized pomeron flux lowers the hard-quark prediction down to 2.8% (6).

A search for diffractive W 's is currently being conducted in the CDF experiment at the Tevatron at $\sqrt{s}=1800$ GeV. In the absence of a roman pot spectrometer, the rapidity gap technique is used to tag diffraction. For non-diffractive (ND) $W(\rightarrow l\nu)$ events, the underlying event is expected to be right-left symmetric in η -space (1800 GeV curve in Fig. 3-*left*), while for diffractive events an asymmetry is expected ($M_X = 200$ and 300 GeV curves in Fig. 3-*left*). Moreover, the diffractive asymmetry is correlated with the sign of the lepton- η and, independently, with the sign of the lepton charge. The lepton- η correlation with the rapidity gap is the result of the diffractive kinematics, while the charge-gap correlation is due to the fact that, because of the high W mass, mainly valence quarks from the quark-flavor asymmetric (anti)proton interact with the flavor-symmetric pomeron. The distributions shown in Fig. 3(*right*) were obtained using the POMPYT Monte Carlo program (8) with a hard-quark pomeron structure function. Monte Carlo studies have shown further that non-diffractive events with a rapidity gap caused by fluctuations in the underlying event multiplicity do not show any correlations between the gap and the angle or the charge of the lepton.

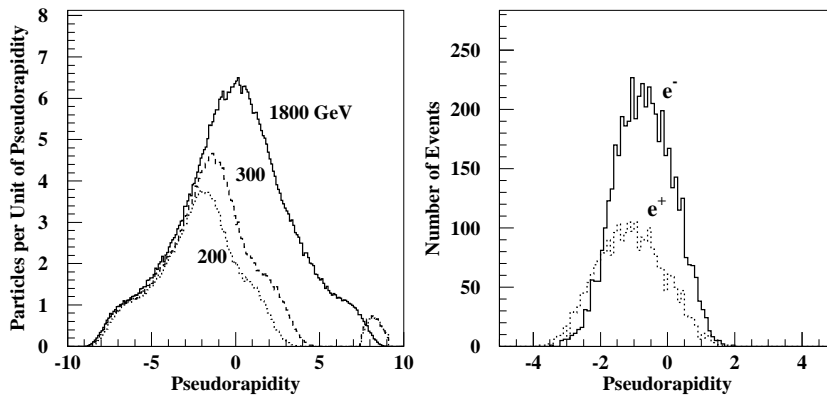


FIG. 3. Monte Carlo generated (*left*) underlying event and (*right*) lepton- η distributions for $p + \bar{p} \rightarrow p + X$; the *recoil* p goes in the positive- η direction.

Experimentally, one looks for events devoid of calorimeter towers with transverse energy $E_T > 200$ MeV in the region $2 < |\eta| < 4.2$, where 4.2 is the maximum instrumented η -value in the CDF detector. Fig. 4(*top*) shows two superimposed tower-multiplicity distributions in the region $2 < |\eta| < 4.2$. The solid histogram is the *correlated* multiplicity, in which the rapidity gap is opposite the lepton- η or for which the (anti)proton is opposite the $(l^+)l^-$, while the dashed histogram represents the *anticorrelated* multiplicity, which has opposite to the above correlations. The events with zero multiplicity (first bin) are diffractive candidates. The fraction of diffractive events among

these candidates is evaluated by comparing the two distributions. Quantitatively, this fraction is equal to the measured asymmetry in the first bin, $A = (N_c - N_{\bar{c}})/(N_c + N_{\bar{c}})$, divided by the asymmetry predicted by the Monte Carlo simulation for diffractive events (see Fig. 3-*right*). This procedure assumes that the asymmetry expected for non-diffractive events in the first bin is zero. That this is the case was verified by Monte Carlo studies, as mentioned above, and can also be inferred from Fig. 4(*bottom*), which shows the asymmetries for all multiplicity bins.

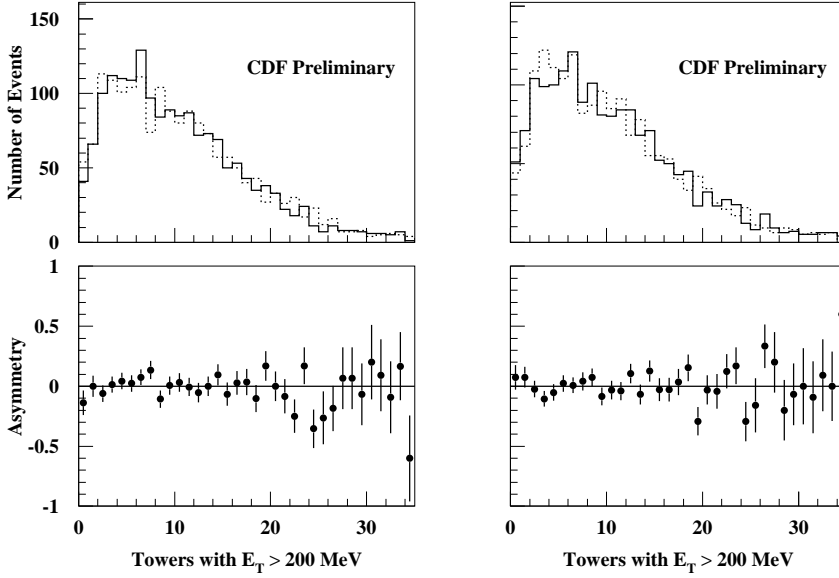


FIG. 4. Charge (left) and angle (right) correlated multiplicity distributions (solid lines) in the region $2.0 < |\eta| < 4.2$ compared with the anti-correlated distributions (dashed lines) for W events; (*bottom*) The asymmetry $A = (N_c - N_{\bar{c}})/(N_c + N_{\bar{c}})$ as a function of multiplicity.

In a sample of $\sim 3,500$ W events analyzed, a fraction of $R_{gap} = (5.8 \pm 0.4)\%$ have a rapidity gap in the region $2 < |\eta| < 4.2$, but the asymmetry analysis shows that only a fraction of $R_{gap}^D = (0.2 \pm 0.8)\%$ of the events can be attributed to diffractive production. To obtain the fraction of all diffractive events in the sample, R^D , the value of R_{gap}^D must be divided by 0.87 to account for calorimeter noise and by the relative acceptance of diffractive events with a gap to all ND events. While the acceptance, which depends on the procedure used to model the underlying event, is currently being evaluated, it will only affect the uncertainty in the measurement as no signal has been observed. Current indications are that $R^D \sim 0 \pm \text{a few } \%$, which should be compared with the BI prediction of 17% and the renormalized flux prediction of 2.8%. An experimental limit of *a few %* restricts the hard-quark structure function

of the pomeron for the BI-type flux, but lacks the sensitivity needed to probe the pomeron structure if the renormalized flux factor is used.

C. Diffractive dijets in CDF

The rapidity gap method was also used in CDF to search for diffractive dijet production, which, as in the UA8 experiment, is sensitive to both the quark and the gluon content of the pomeron. Because of the higher energy of the Tevatron, dijets in the same diffractive mass-region as UA8, $M_X^2 \sim 150 \text{ GeV}^2$, are produced with lower pomeron ξ , since $\xi \approx M_X^2/s$. The signature for such events is two high- P_T jets on the same side of the rapidity region and a rapidity gap on the other side. Since the rapidity gap method integrates over t , and because of the exponential t -behavior of the diffractive cross section, the average t -value of the events in CDF is close to zero, in contrast to UA8 for which $|t| \sim 1.5 \text{ GeV}^2$. Probing the structure of the pomeron with the same hard process but different pomeron ξ and t can address the question of the uniqueness of the pomeron structure.

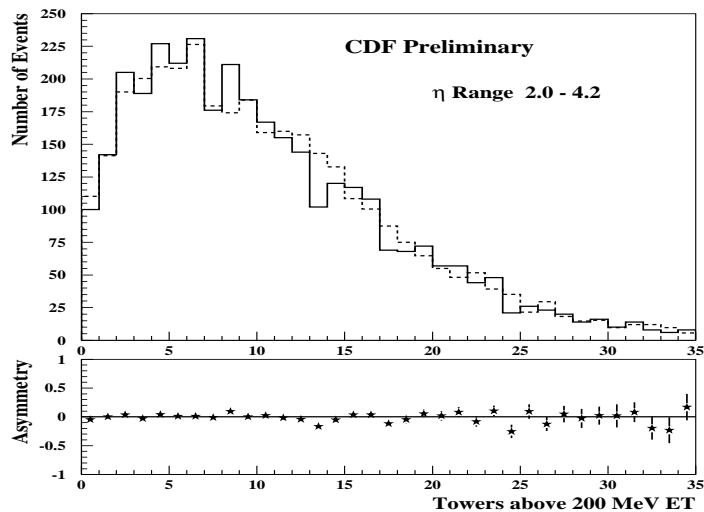


FIG. 5. (*top*) Multiplicity distribution in the region $2.0 < |\eta| < 4.2$ opposite the dijet (solid line) or the lepton from W-decay (dashed line); (*bottom*) The asymmetry $A = (N_{jj} - N_W)/(N_{jj} + N_W)$ as a function of multiplicity.

A sample of 3415 events with two jets of $P_T > 20 \text{ GeV}$ and $|\eta| > 1.8$ was analysed. As in the W analysis, one looks for events devoid of calorimeter towers with $E_T > 200 \text{ MeV}$ in the region $2 < |\eta| < 4.2$. The multiplicity distribution for the region *opposite* the dijet for all events is plotted in Fig. 5(*top*) and compared with the same distribution for the W-sample normalized to the same number of events. The two distributions agree in all multiplicity bins, including the bin of zero multiplicity, as shown quantitatively in Fig. 5(*bottom*).

The W -distribution has two entries per event, one for each side of the rapidity region. Therefore, the measured fraction of $(0.2 \pm 0.8)\%$ diffractive W -candidates in this sample goes down to $(0.1 \pm 0.4)\%$ diffractive gaps, and since there are approximately twice as many W as dijet entries, the number of diffractive rapidity gap candidates in the W -sample becomes $(0.05 \pm 0.2)\%$ of the dijet events. The dijet-sample contains 3% rapidity gap events, but the excess of such events over the W -sample is found to be -10 ± 13 , which corresponds to $(-0.30 \pm 0.37)\%$ of the events. Because of the negative value obtained, even if there were diffractive rapidity gap events at the level of the 0.2% uncertainty estimated above, correcting for them would bring the measured value closer to zero but would not affect the upper limit set by the error of $\pm 0.37\%$. The 95% CL upper limit obtained for the ratio of diffractive to ND dijets with a rapidity gap is $R_{gap} < 0.6\%$, which corrected for calorimeter noise and for the relative diffractive to ND acceptance becomes $R(\frac{D}{ND}) < 0.75\%$. This value is to be compared with $\sim 5\%$ predicted from POMPYT for standard flux diffractive and from PYTHIA for ND dijets, and with $\sim 0.6\%$ obtained using the renormalized flux. The corresponding limits on the discrepancy factor for a full hard-gluon pomeron structure function is 0.14 for the standard flux, and 1.2 for the renormalized flux. Again, while this measurement limits severely the hard-gluon pomeron structure function for the standard flux, at this level of accuracy it is not a sensitive probe of the pomeron structure if the renormalized flux is used.

III. DEEP INELASTIC DIFFRACTION AT HERA

At HERA, the quark content of the pomeron is probed directly with virtual high- Q^2 photons in e^-p deep inelastic scattering at $\sqrt{s} \sim 300$ GeV (28 GeV electrons on 820 GeV protons). Both the H1 (9) and ZEUS (10) Collaborations have reported measurements of the diffractive structure function $F_2^D(Q^2, \xi, \beta)$ (integrated over t , which is not measured), where β is the fraction of the pomeron's momentum carried by the quark being struck. The experiments find that the ξ -dependence factorizes out and has the form $1/\xi^{1+2\epsilon}$, which is the same as the expression in the pomeron flux factor (see Eq. 1). Moreover, the fits yield $\epsilon \approx 0.1$, which is in agreement with the value measured in *soft* collisions.

In this paper we evaluate the pomeron structure function from the H1 results using the renormalized pomeron flux (11) (a similar analysis could be done on the ZEUS results). For fixed Q^2 and β , $\xi_{min} = (Q^2/\beta s)$. Therefore, the flux integral, which to a good approximation varies as $\xi_{min}^{-2\epsilon}$, is given by

$$N(\xi_{min}) = N(s, Q^2, \beta) \approx \left(\frac{\beta s}{Q^2} \xi_0 \right)^{2\epsilon} = 3.8 \left(\frac{\beta}{Q^2} \right)^{0.23} \quad (3)$$

where ξ_0 is the value of ξ_{min} for which the flux integral is unity. For our numerical evaluations we use $\sqrt{s}=300$ GeV and the flux factor of Ref. (6), in

which $\epsilon = 0.115$. The value of ξ_0 turns out to be $\xi_0 = 0.004$.

H1 integrates the diffractive form factor $F_2^D(Q^2, \xi, \beta)$ over ξ and provides values for the expression

$$\tilde{F}_2^D(Q^2, \beta) = \int_{0.0003}^{0.05} F_2^D(Q^2, \xi, \beta) d\xi \quad (4)$$

The pomeron structure function is related to $\tilde{F}_2^D(Q^2, \beta)$ by factorization:

$$\tilde{F}_2^D(Q^2, \beta) = \left[\frac{\int_{0.0003}^{0.05} d\xi \int_0^\infty f_{\mathcal{P}/p}(\xi, t) dt}{N(s, Q^2, \beta)} \right] F_2^{\mathcal{P}}(Q^2, \beta) \quad (5)$$

The expression in the brackets is the normalized flux factor. The integral in the numerator has the value 2.0 when the flux factor of (6) is used. Assuming now that the pomeron structure function receives contributions from the four lightest quarks, whose average charge squared is $5/18$, the quark content of the pomeron is given by

$$f_q^{\mathcal{P}}(Q^2, \beta) = \frac{18}{5} F_2^{\mathcal{P}}(Q^2, \beta) \quad (6)$$

The values of $f_q^{\mathcal{P}}(Q^2, \beta)$ obtained in this manner are shown in Fig. 6.

As seen, the renormalized points show no Q^2 dependence. We take this fact as an indication that the pomeron *reigns in the kingdom of asymptopia* and compare the data points with the asymptotic momentum fractions expected for any quark-gluon construct by leading-order perturbative QCD, which for n_f quark flavors are

$$f_q = \frac{3n_f}{16 + 3n_f} \quad f_g = \frac{16}{16 + 3n_f} \quad (7)$$

The quark and gluon components of the pomeron structure are taken to be $f_{q,g}^{\mathcal{P}}(\beta) = f_{q,g} [6\beta(1 - \beta)]$. For $n_f = 4$, $f_q = 3/7$ and $f_g = 4/7$. The pomeron in this picture is a combination of valence quark and gluon color singlets and its complete structure function, which obeys the momentum sum rule, is given by

$$f^{\mathcal{P}}(\beta) = \frac{3}{7}[6\beta(1 - \beta)]_q + \frac{4}{7}[6\beta(1 - \beta)]_g \quad (8)$$

The data in Fig. 6 are in reasonably good agreement with the quark-fraction of the structure function given by $f_q^{\mathcal{P}}(\beta) = (3/7)[6\beta(1 - \beta)]$, except for a small excess at the low- β region. An excess at low- β is expected in this picture to arise from interactions of the photon with the gluonic part of the pomeron through gluon splitting into $q\bar{q}$ pairs. Such interactions, which are expected to be down by an order of α_s , result in an *effective* quark β -distribution of the form $3(1 - \beta)^2$. We therefore compare in Fig. 6 the data with the distribution

$$f_{q,eff}^{\mathcal{P}}(\beta) = (3/7)[6\beta(1 - \beta)] + \alpha_s(4/7)[3(1 - \beta)^2] \quad (9)$$

using $\alpha_s = 0.1$. Considering that this distribution involves *no free parameters*, the agreement with the data is remarkable!

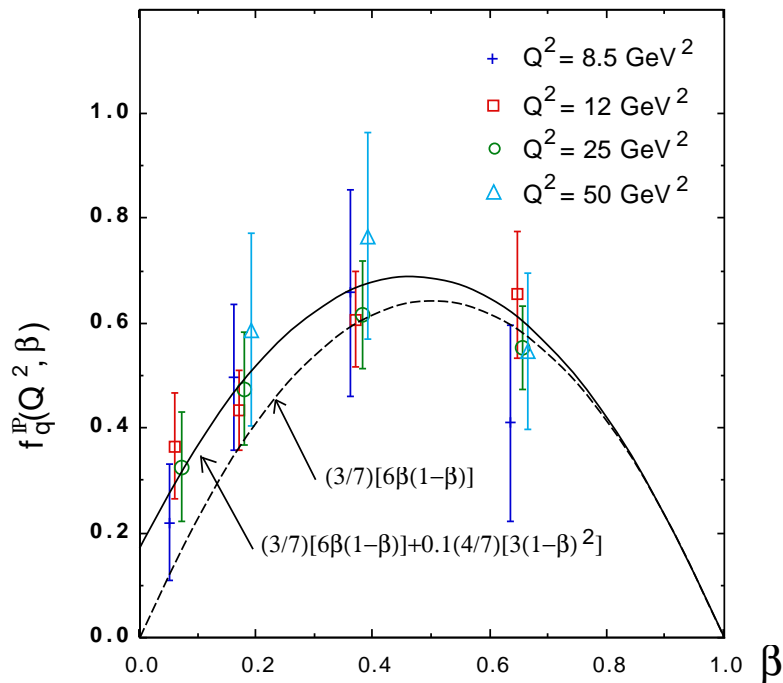


FIG. 6. The quark component of the pomeron seen in DIS is compared to the prediction (solid line) based on four quark flavors and a pomeron that obeys the momentum sum rule; the dashed line represents the direct quark contribution.

IV. SUMMARY AND CONCLUSIONS

We have reviewed the experimental measurements on hard diffraction at hadron colliders and on deep inelastic scattering with large rapidity gaps at HERA. Using the standard pomeron flux, the quark component of the pomeron at HERA has a rather flat β -distribution (9,10) and integrates out to an average value of $\bar{f}_q \sim 1/3$. In contrast, UA8 finds a hard structure with a small amount of soft component, if any; also, a $1/3$ quark component would almost saturate the UA8 rate, leaving little room for a gluon component in the pomeron. Coming now to the CDF results, with such a structure one would predict a diffractive W rate of $\sim 6 - 8\%$, depending on the flux parametrization, which is to be compared with a null result of *a few %* accuracy. Thus, the standard flux presents a picture of a mostly quark-made pomeron with a different momentum sum rule discrepancy factor for HERA, UA8 and CDF.

Flux renormalization restores order by presenting us with a pomeron that obeys the momentum sum rule and satisfies all present experimental constraints. This pomeron consists of a combination of valence quark and gluon color singlets in a ratio suggested by asymptopia for four quark flavors. In

detail, the results obtained with this model are:

- No free parameters are needed to fit the HERA data (see Fig. 6).
- HERA and UA8 both find a predominantly hard structure with a small soft component, which can be accounted for by gluon-splitting into $q\bar{q}$ pairs or gluon radiation by the quarks of the pomeron.
- For a pomeron consisting of 3/7 quark and 4/7 gluon hard components, the discrepancy factor for UA8 becomes $1.19 \pm 0.18 \pm 0.61$, which is consistent with unity and therefore in agreement with the momentum sum rule.
- The diffractive W production fraction at the Tevatron is predicted to be 1.2%. This value is not in conflict with the CDF null result of a few % accuracy.
- The diffractive dijet fraction at the Tevatron for jet $|\eta| > 1.8$ and $P_T > 20$ GeV is predicted to be $\sim 0.5\%$, which is also not in conflict with the CDF measurement.

In conclusion, the pomeron structure function given by Eq. (8) accounts for all present experimental results when used in conjunction with the renormalized flux of (6).

REFERENCES

1. K. Goulianos, Physics Reports **101** (1983) 169.
2. G. Ingelman and P. Schlein, Phys. Lett. **B152** (1985) 256.
3. A. Brandt et al. (UA8 Collaboration), Phys. Lett. **B297** (1992) 417;
R. Bonino *et al.* (UA8 Collaboration), Phys. Lett. **B211** (1988) 239.
4. P. Schlein, *Evidence for Partonic Behavior of the Pomeron*, Proceedings of the International Europhysics Conference on High Energy Physics, Marseille, France, 22-28 July 1993 (Editions Frontieres, Eds. J. Carr and M. Perrottet).
5. A. Donnachie and P. Landshoff, Nucl. Phys. **B303** (1988) 634.
6. K. Goulianos, *Pomeron flux renormalization in soft and hard diffraction*, Rockefeller U. Preprint **RU 95/E-06, Revised May 5, 1995**; *ib.*, HEP-PH-9502356.
7. P. Bruni and G. Ingelman, *Phys. Lett.* **B311** (1993) 317.
8. P. Bruni and G. Ingelman, POMPYT version 1.0, *A Monte Carlo to Simulate Diffractive Hard Scattering Processes*, DRAFT, DESY, November 15, 1993.
9. H1 Collaboration, *First Measurement of the Deep-Inelastic Structure of Proton Diffraction*, DESY 95-36 (February 1995).
10. ZEUS Collaboration, *Measurement of the diffractive structure function in deep inelastic scattering at HERA*, DESY 95-093 (May 1995).
11. *The Structure of the Pomeron*, Rockefeller University Preprint RU 95/E-26, May 15, 1995; *ib.*, HEP-PH-9505310.